The Astrophysical Journal, 682:896–906, 2008 August 1

THE DETECTION OF A RED SEQUENCE OF MASSIVE FIELD GALAXIES AT $z \sim 2.3$ AND ITS EVOLUTION TO $z \sim 0$[1]

Mariska Kriek,[2,3] Arjen van der Wel,[4] Pieter G. van Dokkum,[5] Marijn Franx,[3] and Garth D. Illingworth[6]
Received 2007 December 22; accepted 2008 April 25

ABSTRACT

The existence of massive galaxies with strongly suppressed star formation at $z \sim 2.3$, identified in a previous paper, suggests that a red sequence may already be in place beyond $z = 2$. In order to test this hypothesis, we study the rest-frame $U - B$ color distribution of massive galaxies at $2 < z < 3$. The sample is drawn from our near-infrared spectroscopic survey for massive galaxies. The color distribution shows a statistically significant (>3 σ) red sequence, which hosts ~60% of the stellar mass at the high-mass end. The red-sequence galaxies have little or no ongoing star formation, as inferred from both emission-line diagnostics and stellar continuum shapes. Their strong Balmer breaks and their location in the rest-frame $U - B$, $B - V$ plane indicate that they are in a poststarburst phase, with typical ages of ~0.5–1.0 Gyr. In order to study the evolution of the red sequence, we compare our sample with spectroscopic massive galaxy samples at $0.02 < z < 0.045$ and $0.6 < z < 1.0$. The rest-frame $U - B$ color reddens by ~0.25 mag from $z \sim 2.3$ to the present at a given mass. Over the same redshift interval, the number and stellar mass density on the high-mass end ($>10^{11}\ M_{\odot}$) of the red sequence grow by factors of ~8 and ~6, respectively. We explore simple models to explain the observed evolution. Passive evolution models predict too-strong $\Delta(U - B)$ and produce $z \sim 0$ galaxies that are too red. More complicated models that include aging, galaxy transformations, and red mergers can explain both the number density and color evolution of the massive end of the red sequence between $z \sim 2.3$ and the present.

Subject headings: galaxies: evolution — galaxies: formation — galaxies: high-redshift

1. INTRODUCTION

Early-type galaxies with quiescent stellar populations form a well-defined color-magnitude or color-mass relation at $z \sim 0$ known as the "red sequence." They are clearly separated from blue star-forming galaxies, which populate a different, less tight sequence called the "blue cloud." While the red sequence is primarily a buildup of massive galaxies, blue galaxies have lower stellar masses (e.g., Kauffmann et al. 2003).

The appearance and evolution of the red sequence provide a powerful method to study the star formation and assembly history of massive galaxies (e.g., Bower et al. 1992; Schweizer & Seitzer 1992; van Dokkum et al. 1998). The red sequence exhibits a tilt and spread which are thought to be primarily driven by metallicity and age differences, respectively (e.g., Faber 1973; Worthey 1994; Kodama & Arimoto 1997; Kodama et al. 1999). Both the shape and the color of the red sequence evolve over cosmic time. Several processes are responsible for this evolution. First, the color gradually reddens due to aging of stellar populations. Second, the red sequence grows through transformations of blue galaxies. These transformations change the mix of properties of red-sequence galaxies and may cause the observed evolution of the red sequence to deviate from the expectations from passive evolution. Third, mergers among red-sequence galaxies change the red-galaxy mass function and may affect the color, slope, and scatter of the red sequence (e.g., Bower et al. 1992). Thus, the evolution of the color, shape, number, and mass density of the red sequence sets direct constraints on the assembly and star formation history of massive, early-type galaxies.

The evolution of the red sequence between $z \sim 1$ and ~0 has been extensively studied for this purpose. Overall, these studies find that the color evolution is consistent with passive evolution (e.g., Bell et al. 2004), the mass on the red sequence doubles in this redshift interval (e.g., Bell et al. 2004; Faber et al. 2007; Arnouts et al. 2007), and the growth at higher masses is attributed to both red mergers and galaxy transformations (e.g., Bundy et al. 2007). As a significant part of the red sequence was already in place at $z \sim 1$, we have to push our studies to higher redshifts to trace the onset and first buildup of the red sequence.

Recent high-redshift studies report the detection of the red sequence up to $z = 2$ (e.g., Arnouts et al. 2007; Cassata et al. 2008). Moreover, developments in near-infrared (NIR) instrumentation have enabled the first spectroscopic confirmations of quiescent galaxies without detected emission lines beyond $z = 2$ (Kriek et al. 2006a, 2006b). In particular, the cross-dispersed mode of the Gemini Near-Infrared Spectrograph (GNIRS; Elias et al. 2006), with a wavelength coverage of 1–2.5 μm, allows systematic studies of massive galaxies at $z \sim 2.3$. Using this instrument we have completed a NIR spectroscopic study of 36 K-selected galaxies at $2 \lesssim z \lesssim 3$. In this paper we use this survey to study the onset and color evolution of the red sequence. The spectroscopic redshifts in combination with the accurate continuum shapes provided by the NIR spectra allow for the first time accurate rest-frame color determinations of quiescent, massive galaxies beyond $z = 2$.

Throughout the paper we assume a ΛCDM cosmology with $\Omega_m = 0.3$, $\Omega_\Lambda = 0.7$, and $H_0 = 70\ \mathrm{km\ s^{-1}\ Mpc^{-1}}$ and a Salpeter (1955) initial mass function (IMF) between 0.1 and 100 $M_{\odot}$. All broadband magnitudes are given in the Vega-based photometric system.

2. DATA

The data used in this work are extracted from our NIR spectroscopic survey for massive galaxies (Kriek et al. 2008). The full

[1] Based on observations obtained at the Gemini Observatory, which is operated by the Association of Universities for Research in Astronomy, Inc., under a cooperative agreement with the NSF on behalf of the Gemini partnership.

[2] H.N. Russell Fellow, Department of Astrophysical Sciences, Princeton University, Princeton, NJ 08544.

[3] Leiden Observatory, Leiden University, NL-2300 RA Leiden, Netherlands.

[4] Department of Physics and Astronomy, Johns Hopkins University, Baltimore, MD 21218.

[5] Department of Astronomy, Yale University, New Haven, CT 06520.

[6] UCO/Lick Observatory, University of California, Santa Cruz, CA 95064.

sample consists of 36 K-bright galaxies observed with GNIRS in cross-dispersed mode (1.0–2.5 μm) between 2004 September and 2007 March (programs GS-2004B-Q-38, GS-2005A-Q-20, GS-2005B-C-12, GS-2006A-C-6, GS-2006B-C-5, and GS-2007A-C-9). The galaxies were originally selected from the Multiwavelength Survey by Yale-Chile (MUSYC; Gawiser et al. 2006; Quadri et al. 2007), which provides us with accurate optical-to-NIR (*UBVRIzJHK*) photometry.

In Kriek et al. (2008) we show that distribution of the rest-frame $U - V$ and observed $R - K$ colors of our spectroscopic sample are representative of a mass-limited sample at $2 < z < 3$. However, we do note that we are biased toward galaxies with brighter K-band magnitudes. Although this mainly reflects the relatively lower redshifts of these galaxies, as explained in detail in Kriek et al. (2008), we might be missing galaxies with higher mass-to-light ratios (M/L). Further details about sample completeness, observations, reduction, and extraction of the spectra can also be found in Kriek et al. (2008).

For this work we use the 28 galaxies within the range $2 < z_{\rm spec} < 3$. Stellar masses and other population properties are derived by stellar population modeling as described in detail in Kriek et al. (2006a, 2008) and given in Table 2 of Kriek et al. (2008). In summary, we fit the spectra together with the broadband optical photometry by Bruzual & Charlot (2003) stellar population models, assuming an exponentially declining star formation history, solar metallicity, the Calzetti et al. (2000) reddening law, and the Salpeter (1955) IMF between 0.1 and 100 $M_{\odot}$. We allow a grid of 41 values for A_V between 0 and 4 mag, 31 values for the characteristic star-forming timescale (τ) between 10 Myr and 10 Gyr, and 24 values for age (not exceeding the age of the universe). Uncertainties on the stellar population properties are derived using 200 Monte Carlo simulations as described in Kriek et al. (2006a, 2008). We leave redshift as a free parameter for galaxies without emission lines. We test the continuum redshifts using the emission-line galaxies in our sample and find an uncertainty in $\Delta z/(1+z)$ of less than 0.019 (Kriek et al. 2008).

Rest-frame $U - B$[7] colors are also determined from the best-fit stellar population models. In the same fashion as for the stellar population properties, confidence levels are derived from Monte Carlo simulations. Hence, the confidence intervals on the rest-frame colors include the uncertainties on the continuum redshifts for galaxies without emission lines. The colors are not measured directly from the spectra, as for several galaxies the U band is not covered completely by the NIR spectrum or the B band falls partly between the J and H atmospheric windows. As our grid allows almost 30,000 different synthetic spectra, we do not expect the colors to converge to certain best-fit templates. Nevertheless, in order to examine whether using best fits may introduce systematics in the derived rest-frame colors, we directly measure the colors from the NIR spectra in combination with the optical broadband photometry. We find no systematic offset between the direct colors and those derived from the best fits.

The unique aspects of this data set are the accurate spectroscopic redshifts, rest-frame colors, and masses. Although broadband photometric studies provide much larger galaxy samples, they lack the accuracy needed for this study.

3. A RED SEQUENCE AT $z \sim 2.3$

3.1. *The Detection of the Red Sequence at* $z \sim 2.3$

Figures 1*a* and 1*b* present rest-frame $U - B$ color versus stellar mass for the $2 < z < 3$ massive galaxy sample. The colors are corrected for redshift differences within the sample, as explained in § 4.2. These corrections are very small ($\sim$0.001) and barely change the appearance of this plot. The distribution of galaxies in Figures 1*a* and 1*b* is striking, as there are many galaxies with similar red colors. In order to test whether a red sequence was already in place at this early epoch, we examine the rest-frame color distribution. But first, we correct the colors for the tilt of the red sequence by assuming the slope of $z = 0$ red sequence (van der Wel et al. 2007). The applied correction has the form

$$(U - B)_M = (U - B) - 0.08(\log M/M_{\odot} - 11.3). \quad (1)$$

The residuals are shown by the black histograms in Figures 1*c* and 1*d*. The distribution exhibits a conspicuous peak at $(U - B) \sim 0.25$ mag. We test the significance of the red sequence by calculating the probability of obtaining this peak when assuming a flat distribution in rest-frame $U - B$ color. If the true distribution is uniform, the probability of finding nine or more galaxies in any one of the three red bins and finding 16 or more galaxies in total with $U - B > 0.1$ is less than 0.001. Thus, the odds of finding the detected red sequence by chance are less than 0.1%. This implies that the detection of the red sequence is significant at the $>3\,\sigma$ level. This all strongly suggests that a red sequence of massive field galaxies was most likely already in place at $z \sim 2.3$.

We determine the location of the peak of the red sequence by fitting a Gaussian to the color distribution. We average over many binning positions to obtain a distribution that is not affected by the particular choice of binning. In order to avoid including blue-cloud galaxies, we restrict the fitting region to all galaxies with $(U - B)_M > (U - B)_{\rm peak} - 0.1$. Hence, this procedures requires a few iterations. The cutoff value of 0.1 mag is chosen because it is twice the scatter in rest-frame $U - B$ color of the local red sequence (see § 4.2). The best fit is indicated in Figures 1*c* and 1*d* (*solid curve*). The peak of the distribution is shown in Figures 1*a* and 1*b* (*orange line*). All galaxies above the dotted line [$(U - B)_M > (U - B)_{\rm peak} - 0.1$] are defined as red-sequence galaxies hereafter.

Our result may seem in disagreement with previous studies, some of which indicate that the red sequence disappears beyond $z = 1.5$ (e.g., Cirasuolo et al. 2007). However, finding a red sequence, as is well known, requires very accurate rest-frame color determinations. The use of a galaxy sample with spectroscopic redshifts and stellar continuum shapes—*and not just photometric information*—enables us to detect a significant red sequence beyond $z = 2$, in contrast to previous studies. Broadband photometry in combination with photometric redshifts with errors of $\Delta z/(1+z) \sim 0.07$ gives random errors of 0.1 mag in rest-frame $U - B$, and systematic errors may play an even larger role. Furthermore, the typical uncertainties on stellar mass and absolute magnitude are a factor of $\sim$2 and $\sim$0.4 mag, respectively (Kriek et al. 2008). Thus, the uncertainties on the location of the individual red-sequence galaxies are larger than the width of the intrinsic red sequence. This implies that photometric studies with errors of $\sim$0.07 in $\Delta z/(1+z)$ are not able to recover a red sequence. Studies that lack spectroscopic redshifts in the relevant redshift range (e.g., Cirasuolo et al. 2007) to calibrate their photometric redshifts most likely have even larger errors in $\Delta z/(1+z)$.

Whereas we do detect a significant red sequence, we find no bimodality in the galaxy distribution. We cannot reliably comment on bimodality, since larger samples over a larger mass range are needed to assess whether the blue galaxies are distinct from the red ones at this epoch. Nonetheless, recent work by Cassata et al. (2008) based on a spectroscopic study over a larger stellar mass range shows that the galaxy bimodality exists at least out to a

[7] Throughout this paper we use the Buser U, B3, and V filters.

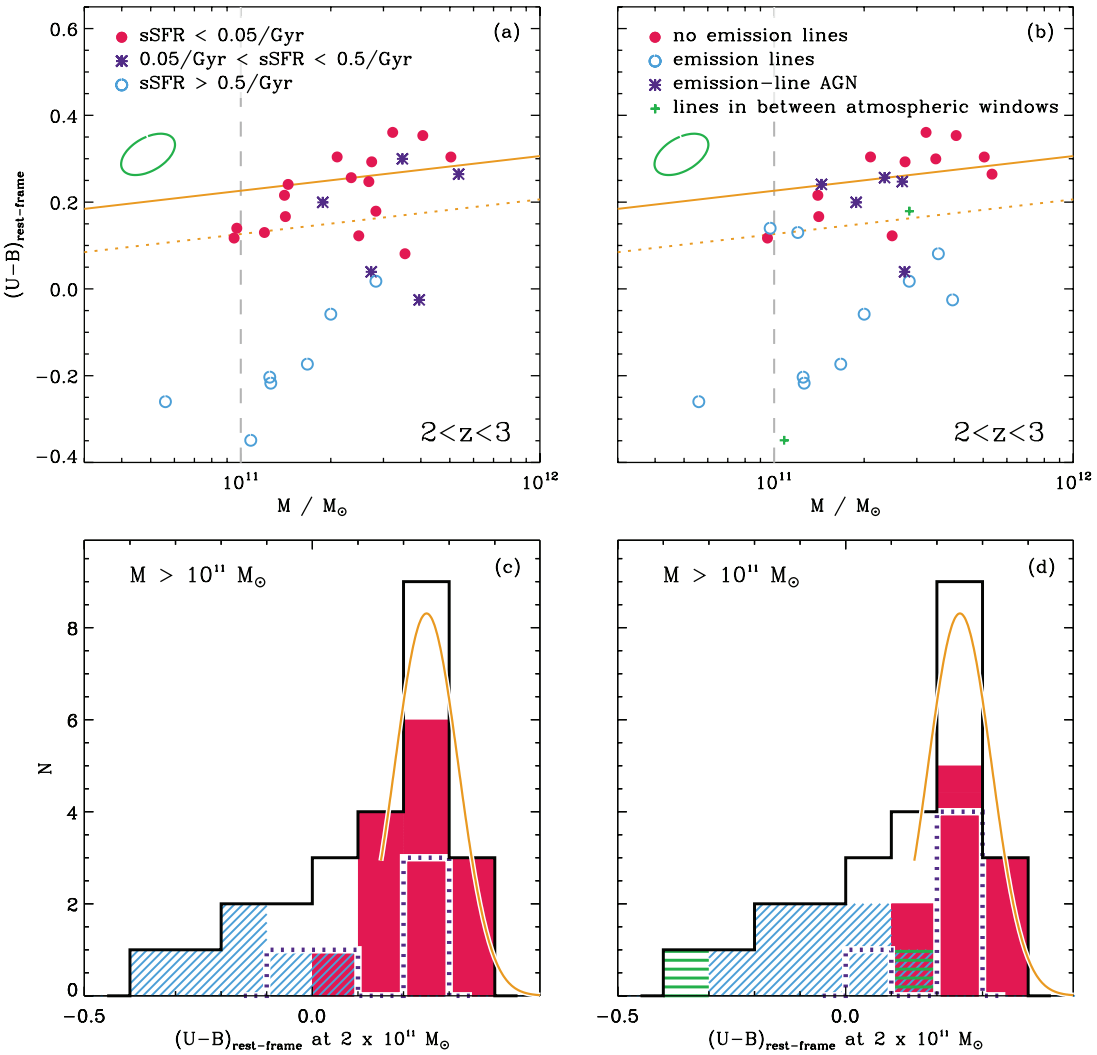

FIG. 1.—Rest-frame $U - B$ vs. stellar mass (*top panels*) and the color distribution at $2 \times 10^{11}\ M_{\odot}$ along the $z \sim 0.0$ slope (*bottom panels*) for the $2 < z < 3$ massive galaxy sample. In the bottom panels we show only galaxies more massive than $10^{11}\ M_{\odot}$ (to the right of the dashed line in the top panels). The black histograms in the bottom panels show a significant peak (>3 σ), indicating that a red sequence was already in place at $z \sim 2.3$. The solid curve in the bottom panels represents the best fit to the color distribution of the red-sequence galaxies. The resulting location of the red sequence is indicated by the solid line in the top panels. All galaxies above the dotted line in the top panels are defined as red-sequence galaxies in this work [$(U - B)_M > (U - B)_{\rm peak} - 0.1$]. The left and right panels illustrate the properties of the galaxies according to SED modeling and emission-line diagnostics, respectively. The symbols in (*a*) indicate the best-fit specific SFRs. In (*b*) the different symbols show whether emission lines are detected for the galaxies and whether the emission lines are dominated by star formation or AGN activity (see Kriek et al. 2007). The corresponding color distributions are presented in (*c*) and (*d*) by the matching colors. The average 1 σ confidence interval is presented by the green ellipse in the top panels. Both independent star formation indicators imply that the red sequence at $z \sim 2.3$ is dominated by galaxies with little or no ongoing star formation.

redshift of $z = 2$. We note that the study by Cassata et al. (2008) is based on spectroscopic redshifts, reinforcing our hypothesis that the current result can only be obtained with redshifts more accurate than the standard photometric redshifts.

Finally, we stress that the detection of a red sequence is independent of whether the sample is fully representative of a mass-limited sample. In this context it is interesting to note that the red sequence was originally discovered and mainly studied in magnitude-limited and not mass-limited samples.

3.2. *Properties of Red-Sequence Galaxies at $z \sim 2.3$*

In the previous section we showed that a red sequence was already in place at $z \sim 2.3$. The well-defined shape of the red sequence could be a consequence of the converging colors of evolved galaxies. However, our sample is small, and dusty starburst galaxies, known to be highly abundant at these redshifts (e.g., Webb et al. 2006; Papovich et al. 2006), may contribute to or even dominate the red sequence at these early epochs. In order to test whether these red-sequence galaxies indeed host quiescent stellar populations, we examine the star formation properties using several diagnostics.

In Figure 1*a* the galaxies are coded following their best-fit specific star formation rate (SFR), derived from modeling their stellar continua (see § 2 and Kriek et al. 2008). The corresponding color distributions are presented in Figure 1*c*. Most red-sequence galaxies are best fit by specific SFRs of less than 0.05 $\rm Gyr^{-1}$, and three have specific SFRs between 0.05 and 0.5 $\rm Gyr^{-1}$. The uncertainties on the specific SFRs are about a factor of 3, on average (Kriek et al. 2008). Nevertheless, the large fraction of galaxies with low specific SFRs suggests that the red sequence is not dominated by dusty starbursts.

A combination of two rest-frame colors, such that one isolates the optical break and the other measures the slope of the spectrum redward of the optical break (e.g., Förster Schreiber et al. 2004;

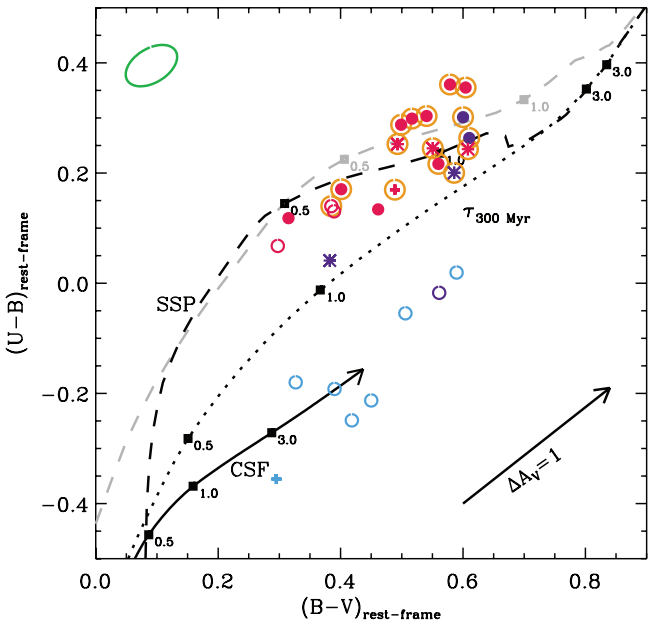

FIG. 2.—Rest-frame $U - B$ vs. $B - V$ for the $2 < z < 3$ massive galaxy sample. The symbols indicate the emission-line diagnostics, as in Fig. 1*b*. The colors indicate the best-fit specific SFRs, similar to the color coding in Fig. 1*a*. The red-sequence galaxies are indicated by the orange open circles. The average 1 σ confidence interval is given at the top left. The black curves show the color evolution tracks of Bruzual & Charlot (2003) models for an SSP (*dashed line*), an exponentially declining model with $\tau = 300$ Myr (*dotted line*), and a CSF model (*solid line*), all for solar metallicity. The dashed gray curve represents an SSP model with $Z = 2.5\ Z_{\odot}$. Ages in Gyr are indicated along the tracks. The vector indicates a reddening of $A_V = 1$ mag for a Calzetti et al. (2000) law. The $B - V$ colors imply that the red-sequence galaxies are in a poststarburst phase.

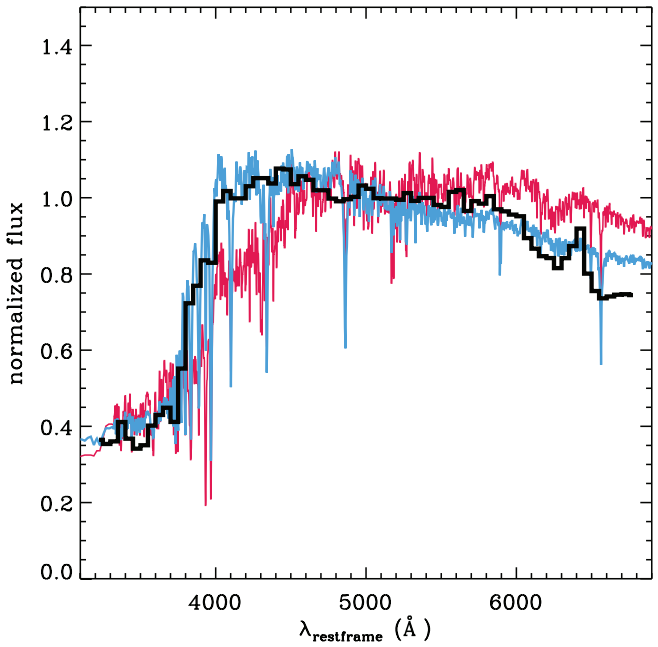

FIG. 3.—Mean stack of the low-resolution GNIRS spectra of the red-sequence galaxies at $z \sim 2.3$ (*black curve*). Overplotted is the mean of all best fits to the spectra in blue. For comparison we show a 2 Gyr SSP model in red. This figure shows that in contrast to the 2 Gyr model, the optical break of the stacked spectrum is dominated by the Balmer break, typical for poststarburst galaxies. This may imply that the red sequence has just started to build up at $z \sim 2.3$.

Labbé et al. 2005; Wuyts et al. 2007), may also be used to discriminate between dusty star-forming galaxies and quiescent stellar populations. In Figure 2 we show rest-frame $U - B$ versus $B - V$ for all galaxies at $2 < z < 3$. Color evolution tracks of the Bruzual & Charlot (2003) models show that quiescent stellar populations have a different locus than dusty starbursts. As expected, the red-sequence galaxies are closer to the simple stellar population (SSP) model tracks. The remaining galaxies can roughly be divided into those that have colors more comparable to constant star-forming (CSF) models with dust and those that will probably soon join the red sequence.

These results are supported by independent emission-line diagnostics, presented in Figures 1*b* and 1*d*. We divide the sample according to whether emission lines are detected in the rest-frame optical spectra. Subsequently, the emission-line galaxies are sorted by the dominant origin of their line emission: using primarily emission-line ratios we discriminate between active galactic nuclei (AGNs) and H II regions (Kriek et al. 2007). For two galaxies we have no information on the line emission, as the lines are expected at wavelengths with low atmospheric transmission. Thirteen out of 15 red-sequence galaxies have no detected emission lines, or the line emission is dominated by AGNs.

Thus, both the stellar continua and the emission-line diagnostics suggest that the red sequence at $z \sim 2.3$ is dominated by galaxies with quiescent stellar populations. In particular, seven out of nine previously identified galaxies with strongly suppressed star formation presented in Kriek et al. (2006b) fall on this red sequence. The rest-frame $U - B$ colors of the two remaining galaxies with strongly suppressed star formation are just below the cutoff value, and their locus in Figure 2 is near the SSP track. Thus, they will most likely soon join the red sequence.

The rest-frame $B - V$ colors in combination with $U - B$ indicate that the red-sequence galaxies at $z \sim 2.3$ are likely in a poststarburst phase (Fig. 2). This is further illustrated in Figure 3, in which we show the stacked low-resolution spectrum of all red-sequence galaxies. For comparison we show a 2 Gyr SSP model with a prominent 4000 Å break as well. In contrast to such old stellar populations, the optical break for the $z \sim 2.3$ red-sequence galaxies is clearly dominated by the Balmer break. Overall, our findings may imply that the massive end of the red sequence is just starting to build up at $z \sim 2.3$ and was likely not yet in place beyond $z \sim 3$. Kodama et al. (2007) drew the same conclusion by studying the stellar populations in protoclusters at $2 \lesssim z \lesssim 3$. Our work is also consistent with the study by Brammer & van Dokkum (2007), who found that in contrast to $z \sim 2.4$, red galaxies at $z \sim 3.7$ have significant UV emission and are thus still actively forming stars. We note, however, that as explained in § 2, we might be missing galaxies with higher M/L, as these are relatively faint in K.

Furthermore, Figure 2 provides us with a clear illustration of the different processes that may be responsible for the spread and tilt of the red sequence at $z \sim 2.3$. A positive correlation of $U - B$ and $B - V$ is shown for the red-sequence galaxies. The typical 1 σ confidence contour shows that random errors cannot fully account for the spread, and other effects are likely to play a role. The two SSP tracks, indicated by the dashed lines in the figure, show that both age and metallicity differences may be responsible for the spread and tilt. Also, the redshift spread of the red-sequence galaxies, corresponding to 0.5 Gyr, will induce scatter in colors. Finally, reddening by dust moves a galaxy in a similar direction as aging and metallicity and may also contribute to the spread and tilt of the red sequence. The importance of the different processes cannot be addressed with the current data, and independent dust, age, and metallicity constraints are required to break the degeneracies.

Finally, we stress that, although star formation activity in the red-sequence galaxies appears low, the galaxies may still be reddened by fair amounts of dust. Best-fit stellar population models indicate an average dust content of $A_V = 0.8$ mag (using the Calzetti reddening law). However, due to degeneracies between age and dust, A_V is poorly constrained, with typical uncertainties of 0.5 mag (Kriek et al. 2008), and dust-free models provide almost equally good fits to the spectra (Kriek et al. 2006b). Metallicity (Z) further complicates this degeneracy, and as it is fixed to $Z_\odot$ during fitting, the lack of appropriate metallicities may be compensated for by adjusting age or A_V. Independent indicators, such as mid-infrared (MIR) imaging or Balmer decrements, are needed to better constrain the dust content in these red-sequence galaxies. MIR imaging also reveals whether obscured star-forming regions may have been missed. In this context it is interesting to note that Reddy et al. (2006a) and Papovich et al. (2006) show that about half of the galaxies at the high-mass end of the galaxy distribution at $z \sim 2.3$ are not detected at 24 μm. Moreover, Reddy et al. (2006a) find that the Hα luminosity for $z \sim 2$ galaxies tracks the bolometric luminosity very well. Finally, large amounts of dust in all red-sequence galaxies studied in this work seems unlikely, because it would then be hard to explain the narrow peak in the observed color distribution.

4. MEASURING THE EVOLUTION OF THE RED SEQUENCE

In order to measure the rest-frame $U - B$ evolution of the red sequence, in this section we compare our $z \sim 2.3$ results with those of lower redshift samples. We use two spectroscopic massive galaxy samples ($>10^{11}\,M_\odot$) at $0.02 < z < 0.045$ and $0.6 < z < 1.0$, extracted from the Sloan Digital Sky Survey (SDSS; York et al. 2000) Data Release 5 (DR5; Adelman-McCarthy et al. 2007) and the Great Observatories Origins Deep Survey (GOODS; Giavalisco et al. 2004), respectively.

4.1. *Spectroscopic Samples at Lower Redshifts*

For our lowest redshift sample we use a complete, mass-selected, volume-limited sample of galaxies at redshifts $0.02 < z < 0.045$ extracted from the SDSS. See van der Wel et al. (2007) for more details about the extraction and completeness of the sample. The SDSS $u - g$ and $g - r$ colors are used to derive rest-frame $U - B$ colors.[8] The M/Ls are derived from the $g - r$ colors (corrected for galactic extinction and redshift) using the relation by Bell et al. (2003). The inferred stellar masses are increased by 0.15 dex to account for differences in the IMF. The final massive ($>10^{11}\,M_\odot$) galaxy sample consists of 903 galaxies.

For the intermediate-redshift sample at $0.6 < z < 1.0$, we use a mass-selected, volume-limited galaxy sample constructed from GOODS-South. A detailed description of the extraction of the sample and completeness can be found in van der Wel et al. (2007). Rest-frame $U - B$ and $B - V$ colors for the $0.6 < z < 1.0$ sample are derived from the F606W, I775W, and F850LP ACS photometry. Subsequently, $B - V$ provides us with stellar masses, using the empirical relations by Bell et al. (2003). Again, the stellar masses are increased by 0.15 dex. Of this sample, 137 galaxies have masses $>10^{11}\,M_\odot$. Spectroscopic redshifts are known for 70% of this sample (Le Fèvre et al. 2004; Mignoli et al. 2005; van der Wel et al. 2005; Vanzella et al. 2006). As this spectroscopic sample is not fully representative of the total sample, we include the galaxies with photometric redshifts (Wuyts et al. 2008) when appropriate.

4.2. *The Color Evolution of the Red Sequence*

For an accurate measurement of the $U - B$ color evolution, it is crucial to derive the color of the red sequence in a fashion similar to that for our $z \sim 2.3$ sample. In Figure 4 (*top panels*) we show rest-frame $U - B$ versus stellar mass for all three massive galaxy samples. The colors are corrected for redshift differences within each subsample in a self-consistent way, by using the evolution of the red-sequence color with time derived below. Next, we subtract equation (1) from the data and determine the peak of the color distribution in the same way as for the $z \sim 2.3$ sample. The extracted color distribution along the $z \sim 0.03$ slope is presented in Figure 4 (*bottom panels*). Galaxies with colors $(U - B)_{M,z} > (U - B)_{\rm peak} - 0.1$ are defined as belonging to the red sequence. The peak locations are indicated by solid lines in Figure 4. For the $0.6 < z < 1.0$ galaxies we exclude the 30% without spectroscopic redshifts when deriving the peak of the red sequence, as these galaxies have less accurate rest-frame colors.

Random errors on the location of the red sequence are determined using bootstrapping and are represented by the dotted lines in the bottom panels of Figure 4. The use of different samples and methods to derive rest-frame colors and stellar masses may introduce additional systematic errors. In order to correctly interpret the observed evolution, we examine the following effects.

Aperture differences.—Elliptical galaxies exhibit color gradients (e.g., Franx & Illingworth 1990). Thus, differences in the apertures that were used to measure rest-frame $U - B$ may introduce systematics in the color evolution. For both the $z \sim 0.03$ and the $z \sim 0.73$ samples the rest-frame $U - B$ colors are derived for an aperture which is about equivalent to the half-light radius. For the $z \sim 2.3$ sample we use the NIR spectra to measure rest-frame $U - B$. The aperture sizes are rectangular and depend on the slit width ($0.675''$), extraction aperture, and extraction method. We use a weighted (with signal-to-noise ratio) extraction and include spatial elements that have a flux larger than 0.25 times the maximum flux (Kriek et al. 2008). Thus, the total aperture size is dependent on the light distribution of the galaxy. The average effective aperture of the $z \sim 2.3$ sample is comparable to a circular aperture of $\sim$8 kpc.

In order to quantify possible systematics in rest-frame $U - B$ determinations of red-sequence galaxies between the $z < 1$ and $z \sim 2.3$ samples, we measure rest-frame $U - B$ for all galaxies in the $z \sim 0.73$ sample using an aperture of $1''$ ($\sim$7.6 kpc at $z \sim 0.73$) instead of $0.5''$. This aperture size is comparable to that used for the $z \sim 2.3$ sample. For the increased aperture the $U - B$ color of the $z \sim 0.73$ red sequence is 0.01 mag bluer. In order to correct for this effect, we have reduced the colors of the $0.02 < z < 0.045$ and $0.6 < z < 1.0$ galaxies by 0.01 mag.

Zero points.—Uncertainties in zero points directly result in systematic uncertainties in the derived rest-frame colors. The uncertainty in individual zero points is <0.01 mag for both the $0.02 < z < 0.045$[9] and $0.6 < z < 1.0$ (Sirianni et al. 2005) samples. Thus, the resulting uncertainty in $U - B$ is <0.02 mag. For the $z \sim 2.3$ sample we use AV 0–type stars for calibrating the spectra. This results in an uncertainty in the rest-frame $U - B$ of $\sim$0.03 mag. For this sample the broadband photometry provides us with an independent check of the zero points. In Kriek et al. (2008) we find a systematic offset of $\sim$0.01 mag between rest-frame $U - V$ derived from the photometry (using $z_{\rm spec}$) and the

[8] The AB-to-Vega zero-point conversions for the U, B, and V bands used in this paper are slightly different from those adopted in van der Wel et al. (2007). The conversions used in this paper are the same as those used by Bruzual & Charlot (2003).

[9] See http://www.sdss.org/.

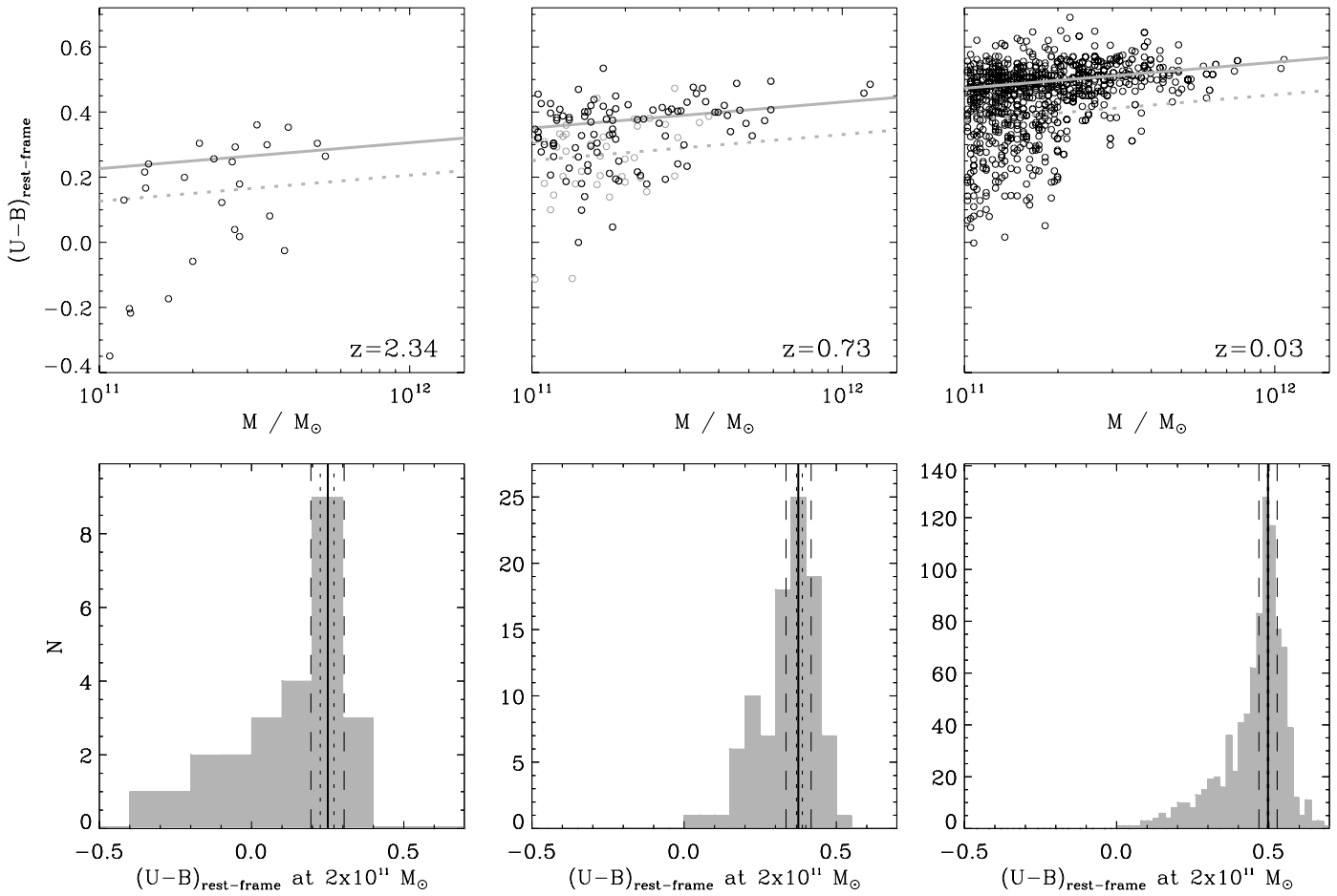

FIG. 4.— *Top panels*: Rest-frame $U - B$ color vs. stellar mass for the three galaxy samples. The two lower redshift samples are adopted from van der Wel et al. (2007). Galaxies without spectroscopic redshifts in the $0.6 < z < 1.0$ sample are indicated in gray. The $U - B$ colors are corrected for redshift differences within the sample using eq. (2). *Bottom panels*: Color distribution extracted along the $z \sim 0.03$ slope (0.08 mag dex^{-1}). The peak of the red sequence is represented by the solid gray and black lines in the top and bottom panels, respectively. All galaxies above the gray dotted lines in the top panels are defined as red-sequence galaxies. The dotted and dashed lines in the bottom panels indicate random and total 1 σ uncertainties, respectively.

NIR spectra. This shows that the zero points probably introduce no large systematics for the $z \sim 2.3$ sample.

Rest-frame color determinations.—The determination of rest-frame colors may also result in systematic errors. For the low- and intermediate-redshift samples we use the photometry in combination with spectroscopic redshifts. This method may result in systematics of $\sim$0.01 and $\sim$0.03 mag for the $0.02 < z < 0.045$ and $0.6 < z < 1.0$ samples, respectively. For the $z \sim 2.3$ sample we have higher resolution spectral shapes provided by the NIR spectra. In the previous paragraph and in § 2 we discuss two tests to assess rest-frame color determinations, and neither of them exhibit significant systematics ($\sim$0.01 mag).

Stellar mass determinations.—Although the stellar masses are all determined for the same IMF, the different methods used for the $z < 1$ and $z \sim 2.3$ samples may have introduced systematic errors. We tested this by determining the stellar masses for the $z \sim 2.3$ galaxies using the same method as for the lower redshift samples. This yielded stellar masses which are typically 0.13 dex less than the best-fit stellar masses. This may be due to younger and dustier stellar populations of the $z \sim 2.3$ massive galaxies. As the slope of the red sequence is 0.08 mag dex^{-1}, this may result in a systematic error of $\sim$0.01 mag on the observed color evolution. Furthermore, this effect may also alter the cutoff value of $10^{11}\,M_{\odot}$ and, consequently, the selection of massive red-sequence galaxies. Increasing the mass cutoff value by 0.13 dex would not change the peak location of the red sequence. However, the number and mass fractions of massive galaxies on the red sequence would increase by $\sim$10%.

Completeness.—The $z \sim 0.03$ sample is volume-limited, and thus completeness effects are not expected to play a role. For the $z \sim 0.73$ sample we use just the spectroscopic subsample to estimate the red-sequence color, as photometric redshifts results in less accurate rest-frame colors. However, including all galaxies would give a rest-frame $U - B$ color which is 0.01 mag less. Thus, completeness effects may result in a systematic error of $\sim$0.01 for the $z \sim 0.73$ sample.

The $z \sim 2.3$ sample is much smaller and not volume-limited. In Kriek et al. (2008) we find that the distributions of rest-frame $U - V$ color, observed $R - K$ and $J - K$ color, and redshift for the spectroscopic sample at $2 < z < 3$ are similar to those of a photometric mass- and volume-limited sample at the same redshift interval. Unfortunately, we can only compare photometric properties in order to investigate whether the subsample is representative, and thus systematics in photometric studies may jeopardize the real completeness. For example, in Kriek et al. (2008) we identified systematics between photometric redshift and SED type, such that dusty, young galaxies were generally placed at too-high redshifts. Because these dusty galaxies scattered to lower redshifts, they were not included in the sample used in this work. Dusty galaxies with $2 < z_{\rm spec} < 3$ may not be properly represented

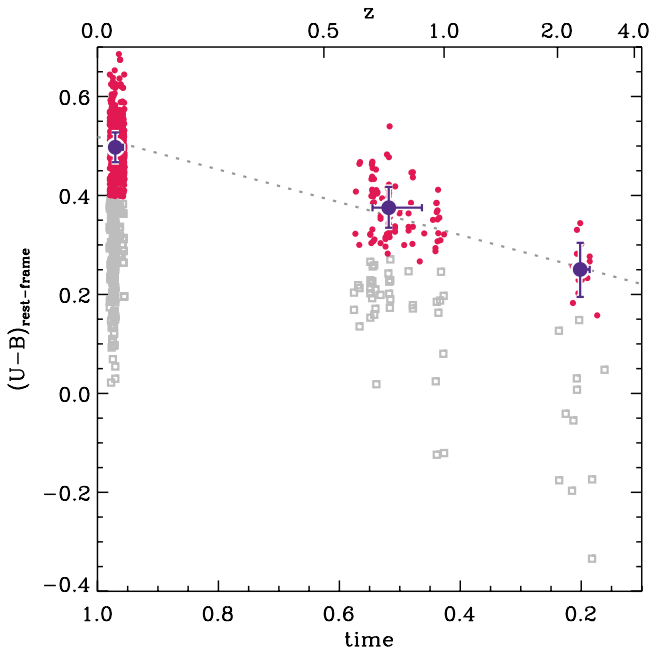

FIG. 5.—$U-B$ color vs. time for all galaxies in the three massive galaxy samples ($>10^{11}\ M_{\odot}$). The rest-frame $U-B$ colors for the individual galaxies in this plot are corrected for the slope in the $U-B$ vs. stellar mass relation (0.08 mag dex^{-1}) and given for a stellar mass of $2\times10^{11}\ M_{\odot}$. The red-sequence galaxies are indicated by the red circles, and the gray squares represent the remaining galaxies. The colors of the red sequence for the three samples are indicated by the purple circles. The dotted line represents the best linear fit through the red-sequence locations. This relation is used to correct $U-B$ colors for redshift differences within the samples.

in the sample, as they were initially placed at too-high redshifts. Although this possible incompleteness may not alter our findings of the color of the red sequence, it should be kept in mind that the sample may not be complete and representative of the total population of $2<z<3$ galaxies. We estimate that completeness effects may result in a systematic error of $\sim$0.03 mag on the rest-frame $U-B$ color of the $z\sim2.3$ red sequence.

The various effects discussed above result in total systematic uncertainties of 0.03, 0.04, and 0.05 mag for the $z\sim0.0$, $\sim$0.7, and $\sim$2.3 red-sequence colors, respectively. We assume that the random and systematic errors are independent and can be added in quadrature.

The color evolution of massive galaxies is shown in Figure 5. The red circles show individual red-sequence galaxies, and the purple circles with error bars show the peak locations for galaxies on the red sequence. The dotted line shows a simple linear fit to the large symbols of the form

$$(U-B)_z = 0.19 + 0.33t, \qquad (2)$$

where t is the fractional age of the universe. The fit was used to apply differential color corrections to account for redshift differences within each sample (see above) and provides a remarkably good fit.

Table 1 lists the rest-frame $U-B$ color and the width of the red sequence for the three samples. The color of the red sequence evolves by $\sim$0.25 mag between $z\sim2.3$ and $\sim$0.0. In § 5 we attempt to explain this evolution using simple models.

4.3. *Evolution of the Mass and Number Density*

In addition to $\Delta(U-B)$, the evolution of the number and mass density of red-sequence galaxies places constraints on the buildup

TABLE 1
PROPERTIES OF THE RED SEQUENCE ($>10^{11}\ M_{\odot}$)

Property	$z\sim0.03$	$z\sim0.73$	$z\sim2.34$
Slope (dex^{-1})	0.08[a]	0.08[b]	0.08[b]
$U-B$ at $2\times10^{11}\ M_{\odot}$	$0.50^{+0.03}_{-0.03}$	$0.38^{+0.04}_{-0.04}$	$0.25^{+0.06}_{-0.06}$
$\sigma_{(U-B)}$	$0.048^{+0.002}_{-0.002}$	$0.055^{+0.011}_{-0.000}$	$0.069^{+0.005}_{-0.010}$
$N_{\rm RS}/N_{\rm total}$	$0.77^{+0.02}_{-0.02}$	$0.71^{+0.04}_{-0.04}$	$0.56^{+0.08}_{-0.12}$
$M_{\rm RS}/M_{\rm total}$	$0.78^{+0.02}_{-0.02}$	$0.77^{+0.03}_{-0.04}$	$0.62^{+0.06}_{-0.11}$
$\rho_N(10^{-4}\ {\rm Mpc}^{-3})$	$8.89^{+1.45}_{-1.46}$	$7.46^{+2.82}_{-2.83}$	$1.11^{+0.37}_{-0.41}$
$\rho_M(10^{8}\ M_{\odot}\ {\rm Mpc}^{-3})$	$1.63^{+0.26}_{-0.27}$	$1.36^{+0.52}_{-0.52}$	$0.26^{+0.07}_{-0.08}$

[a] Adopted from van der Wel et al. (2007).
[b] $z\sim0.03$ slope assumed.

of the red sequence. The densities for the $z<1$ samples follow directly from the used samples, as both are volume-limited. To obtain the relative fractions at $z\sim0.73$ we use the full $0.6<z<1.0$ sample, including galaxies with photometric redshifts, in combination with the red-sequence location as derived from the spectroscopic sample.

The galaxies at $2<z<3$ do not form a complete sample. We use the MUSYC deep survey (1030, 1256, and HDF-South; Quadri et al. 2007) to estimate the total number of massive galaxies ($>10^{11}\ M_{\odot}$) at $2<z<3$ (see § 2). Note that most galaxies of our spectroscopic sample are extracted from this survey. We correct the obtained density for systematics in photometric redshifts as derived in Kriek et al. (2008). We find a total number density of massive galaxies of $\rho(M>10^{11}\ M_{\odot})=2.0\times10^{-4}$ Mpc^{-3}. This value is consistent with the values found by van Dokkum et al. (2006) of $(2.2\pm0.6)\times10^{-4}$ Mpc^{-3} and by Drory et al. (2005) of $\sim1.8\times10^{-4}$ Mpc^{-3} for the same mass cut and IMF. Subsequently, we use the mass and number fractions as estimated from the spectroscopic sample to derive the mass and number densities of red-sequence galaxies. We find a number density of massive red-sequence galaxies at $z\sim2.3$ of $(1.1\pm0.4)\times10^{-4}$ Mpc^{-3}.

All number and mass densities are given in Table 1. The uncertainties on the fractions are determined by bootstrapping (see § 4.2). For the number and mass densities, the uncertainties include cosmic variance, random errors, uncertainties on the fractions, and uncertainties introduced by different stellar mass estimators. The *fraction* of the total massive galaxy population that is on the red sequence has evolved by only $\sim$20% from $z\sim2.3$ to the present. Similarly, the fraction of the total stellar mass in galaxies with $M>10^{11}\ M_{\odot}$ that is on the red sequence has evolved by $\sim$15%. However, the total number and mass of red sequence galaxies have increased by factors of $\sim$8 and $\sim$6, respectively, over this time interval.

4.4. *Comparison with Other Studies*

In this section we discuss our results in the context of other studies that investigated the evolution of the red sequence. However, when comparing our findings to these studies, it is important to keep in mind the difference in sample selection and red-sequence definition. For example, Shapley et al. (2005) and Reddy et al. (2006b) find no red-sequence galaxies among their $z\sim2$ Lyman break galaxies (LBGs; Steidel et al. 1996a, 1996b), as the galaxies are selected by their bright optical flux, and thus they only target star-forming galaxies. Only 20% of a mass-limited sample would be identified by LBG selection, and thus this selection technique is not suitable for obtaining unbiased mass-limited samples (van Dokkum et al. 2006).

Using a mass-limited sample with a wide variety of data over a total field of 1.53 deg^2, Conselice et al. (2007) find that the

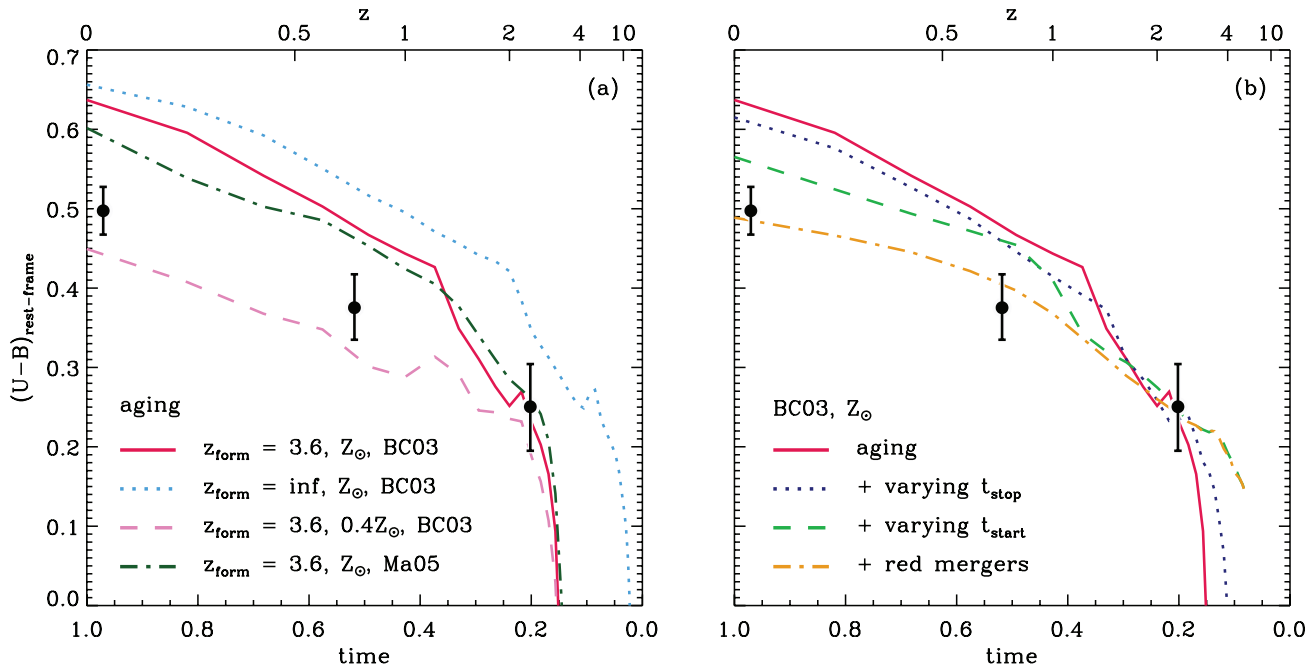

FIG. 6.—Comparison of the observed rest-frame $U - B$ color evolution (*circles*) of the red sequence (at $2 \times 10^{11}\ M_\odot$) with simple models. In (*a*) we examine whether the observations are consistent with passive evolution. The solid and dash-dotted lines show the rest-frame $U - B$ color evolution for SSP models by Bruzual & Charlot (2003) and Maraston (2005), respectively. Both tracks assume solar metallicity and $z_{form} = 3.6$. For comparison we also show an SSP model for an infinite-formation redshift (*dotted curve*) and subsolar metallicity (*dashed curve*), both by Bruzual & Charlot (2003). The evolution is reasonably well fitted by an SSP model with subsolar metallicity. However, this is irreconcilable with current studies of the metallicity of massive elliptical galaxies. In (*b*) we examine more complicated models. The dotted curve represents a model in which the red sequence grows by newly quenched galaxies. The galaxies have the same t_{start} but a different burst length. In the model represented by the dashed line we vary t_{start} as well. In the model represented by the dash-dotted line the evolution is further flattened due to red mergers. The combination of all effects provides a good fit to the observed data.

red-sequence fraction of galaxies with $10^{11}\ M_\odot < M_* < 10^{11.5}\ M_\odot$ increases from 0.65 to 0.88 between $z \sim 1.4$ and $\sim$0.4. Direct comparison with our work is complicated by the different mass range, adopted IMF (Chabrier 2003), and color criteria to identify red-sequence galaxies. Nevertheless, the slight decrease of this fraction may be consistent with the findings presented in this work.

Our study is also broadly consistent with the results of Fontana et al. (2004), who find that $\sim$30%–40% of the present-day stellar mass in objects with $5 \times 10^{10}\ M_\odot < M_* < 5 \times 10^{11}\ M_\odot$ appears to be in place at $z \sim 2$. We find that for $M_* > 1 \times 10^{11}\ M_\odot$, 20% of the mass was already in place at a slightly higher redshift of $z \sim 2.3$. Given the large uncertainties of both studies, the different mass cuts, and the different targeted redshift range, these results are not in conflict with each other. Their relative fraction of red-sequence to blue-sequence galaxies is difficult to compare to ours, as Fontana et al. (2004) have spectroscopic redshifts and classifications for 43% of the galaxies at $1.3 < z < 2.0$. Of these, 21% are early types and 22% are late types. So, for more than half of the sample, the nature of the galaxy is unknown. As late types are easier to spectroscopically confirm (especially with optical spectroscopy) than early types, it is not unlikely that the early types span the majority at this redshift range. Thus, their result is not inconsistent with the fractions we find for our spectroscopic sample at $z \sim 2.3$.

Cirasuolo et al. (2007) find that less than half of the galaxies exceed their red-sequence cut. However, these authors use a *K*-selected, instead of a mass-limited, sample. Higher fractions of blue galaxies are found using *K*-selection, as such galaxies are brighter in *K* than red galaxies at the same stellar mass. Also, since their color distribution shows no obvious peak, their definition of red-sequence galaxies cannot be directly compared to ours.

Finally, Cassata et al. (2008) identify color bimodality out to $z = 2$. Their sample has a spectroscopic completeness of 50%, with 190 spectroscopic redshifts beyond $z = 1.4$. The authors show that early-type galaxies make up 50% of the population at the high-mass end at $z = 2$. When imposing the same color and mass cut as used in this work to their paper, we find that red-sequence galaxies dominate. Furthermore, in agreement with our study, they find that the rest-frame $U - B$ color evolves by only $\sim$0.2 mag between $z \sim 2.5$ and $\sim$0.5.

In summary, it is difficult to directly compare our results with other studies, as few in the targeted redshift range use mass-limited samples. Even more importantly, as discussed in § 3.1, the lack of spectroscopic information prevents accurate rest-frame color determinations of red galaxies for current $z > 2$ studies. Nevertheless, our study seems broadly consistent with other work.

5. MODELING THE EVOLUTION OF THE RED SEQUENCE

In the previous section we derived the evolution of rest-frame $U - B$ color and the number density for the massive end ($>10^{11}\ M_\odot$) of the red sequence between $z \sim 2.3$ and the present. In this section we attempt to explain this evolution using simple models.

5.1. *Aging of Stellar Populations*

The red-sequence galaxies at $z \sim 2.3$ have very little or no ongoing star formation and thus are expected to evolve passively over time. Therefore, simple aging of stellar populations seems to be the most straightforward explanation for the observed color evolution. In Figure 6*a* we compare the measured $U - B$ color evolution to single-burst, solar metallicity models by both Bruzual & Charlot (2003) and Maraston (2005). In § 3 we determine that

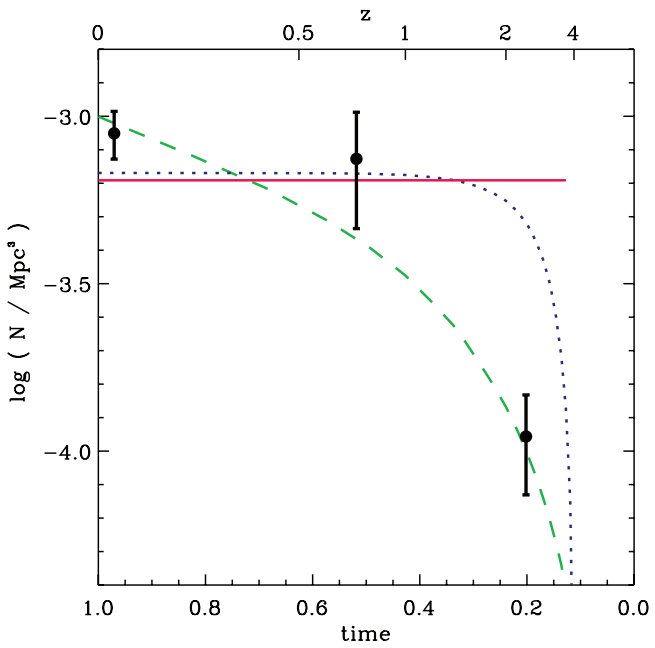

FIG. 7.—Evolution of the number density of red-sequence galaxies more massive than $10^{11}\ M_{\odot}$ (for a Salpeter IMF). The evolution tracks correspond to the models in Fig. 6*b*. Simple aging models (*solid line*) do not match the evolution. The observed evolution is well fitted by models with exponentially declining $t_{\rm start}$ and $t_{\rm stop}$ (*dashed curve*; $\tau_{\rm start} = 1$ Gyr and $\tau_{\rm stop} = 1$ Gyr). Also, models with a large value for $\tau_{\rm stop}$ and a small value for $\tau_{\rm form}$, or the other way around, would provide good fits. The effects of red mergers on the number density evolution are ignored in this figure.

the $z \sim 2.3$ galaxies are in a poststarburst phase, with typical ages of $\sim$0.5 and $\sim$1 Gyr for dust and dust-free models, respectively (Kriek et al. 2006b, 2008). Therefore, we assume a formation redshift of the stars of $z_{\rm form} = 3.6$. For comparison we also give a subsolar model ($0.4\ Z_{\odot}$) and a model with infinite formation redshift, both from the Bruzual & Charlot (2003) library.

Figure 6*a* shows that passive stellar population models with $z_{\rm form} = 3.6$ and solar metallicity predict a too-strong color evolution and produce galaxies at $z \sim 0$ that are too red. Only subsolar models can explain the observed evolution at $2 \times 10^{11}\ M_{\odot}$. However, this is in contradiction to studies of local ellipticals with similar stellar masses, which imply solar to supersolar metallicities (e.g., Worthey et al. 1992).

Perhaps more importantly, passive evolution models do not predict any evolution in the density of galaxies on the red sequence, in clear conflict with the observations (see Fig. 7, *solid line*). Therefore, the evolution of the red sequence is more complicated than just aging. In the following sections we discuss different processes that may have depressed the color evolution.

5.2. *Growth of the Red Sequence by Transformations*

Not all galaxies stop forming stars at high redshift, and the red sequence will be constantly supplemented by newly quenched galaxies. Galaxies that move to the red sequence at later times will be bluer than galaxies that already reside on the red sequence and subsequently will flatten the total color evolution. This effect is known as the "progenitor bias" (van Dokkum & Franx 2001). Qualitatively, such models can reduce the apparent color evolution while there is rapid density evolution and a constant influx of relatively young galaxies to the red sequence.

We apply a simple model in order to test whether including progenitor bias can explain the observed evolution. We assume a formation period of 100 Myr around $z_{\rm form}$ in which all galaxies are formed. The individual galaxies are quenched at $t_{\rm stop}$, following the probability distribution of $\tau_{\rm stop}$,

$$P(t_{\rm stop}) \propto \exp(-t/\tau_{\rm stop}). \quad (3)$$

We use Bruzual & Charlot (2003) models to construct the composite evolution from the color evolution of individual galaxies. We simulate 10,000 galaxies and determine the red-sequence color using the same method as used for the data (see § 4.2). In contrast to van Dokkum & Franx (2001), we assume a constant SFR between $t_{\rm start}$ and $t_{\rm stop}$.

In Figure 6*b* we examine whether the supply of newly quenched galaxies can explain the observed $U - B$ evolution. The dotted curve represents the evolution of an exponentially declining quenching model ($\tau_{\rm stop} = 1$ Gyr). The formation time has been set such that, consistent with the observations, the $z \sim 2.3$ red-sequence galaxies have stopped forming stars for $\sim$1 Gyr ($z_{\rm form} = 4.7$). This model reduces $\Delta(U - B)$ compared to just aging (*solid line*), but it matches neither the observed color nor the number density evolution (see Fig. 7).

One way to further decline the color evolution and better match the observed number density evolution is to increase $\tau_{\rm stop}$ to infinity. However, a more realistic model would be to vary $t_{\rm start}$ in addition to $t_{\rm stop}$. We define the probability distribution of the formation time of the galaxies as

$$P(t_{\rm start}) \propto \exp(-t/\tau_{\rm start}). \quad (4)$$

The dashed curve in Figure 6*b* represents the model with exponentially declining formation and quenching rates ($\tau_{\rm start} = 1$ Gyr and $\tau_{\rm stop} = 1$ Gyr). Also for this model we assume a minimum formation redshift such that, on average, red-sequence galaxies at $z \sim 2.3$ quenched their star formation 1 Gyr ago ($z_{\rm form} = 12$). This model provides a better fit to $\Delta(U - B)$ than the previous two models and matches the evolution of the number density of massive red-sequence galaxies (see Fig. 7). Nonetheless, the predicted color evolution for $2 \times 10^{11}\ M_{\odot}$ red-sequence galaxies is still too slow, and other processes may be needed to match the color evolution. We note, however, that the stellar population models by Maraston (2005) would have provided a slightly better fit to the observed color evolution.

5.3. *Red Mergers*

Mergers on the red sequence may also alter the color evolution (e.g., Bower et al. 1998). Assuming that no star formation is triggered or other major processes take place, merging of two red-sequence galaxies increases the stellar mass but leaves the color unchanged. Thus, red galaxy mergers shift the red sequence to higher masses and consequently reduce the color evolution when measured at fixed mass.

The dash-dotted curve in Figure 6*b* represents the color evolution including red mergers, in addition to aging and a varying $t_{\rm start}$ and $t_{\rm stop}$. We assume a constant merger rate, normalized such that red-sequence galaxies experience one equal-mass merger between $z \sim 1$ and the present. Figure 6*b* shows that the combined model provides a reasonable fit to the observed evolution. If we ignore galaxy transformations, we need five to seven major mergers between $z \sim 2.3$ and the present to provide a good fit to the observed color evolution.

Observational evidence for red mergers (e.g., van Dokkum 2005; Tran et al. 2005; Bell et al. 2006; White et al. 2007) validates this explanation. However, the corresponding decline in the

rest-frame $U - B$ color evolution in this study might be overestimated. First, our assumed merger rates between $z \sim 1$ and ~ 0 may be too high, as accurate observational constraints are still lacking. Furthermore, not all major mergers are equal-mass mergers; for example, a 3 : 1 merger [$\Delta(U - B) = 0.020$ mag] has less impact on the evolution than a 1 : 1 merger [$\Delta(U - B) = 0.024$ mag].

The effects of red mergers on the number density evolution are difficult to estimate using the simple models presented in this work. The merger rate may be dependent on mass, and accurate mass functions are needed to understand the growth of the red sequence due to red mergers (see Bundy et al. 2007).

5.4. *Other Influences*

Although a combination of aging, quenching, and red mergers provides a good fit to observed evolution, there may be other possible explanations as well. One concern is the unknown dust content of red-sequence galaxies, especially at $z \sim 2.3$. The well-defined shape of the $z \sim 2.3$ red sequence makes large dust contents implausible. However, as these galaxies recently stopped forming stars, they may still be in the process of losing their dust. The red-sequence galaxies have a median best-fit A_V of 0.8 mag, but the constraints are poor, with typical 1 σ errors of 0.5 mag. Furthermore, as explained in § 3.2, the degeneracy with metallicity may introduce an additional systematic error. Nonetheless, an A_V of 0.8 mag would lower the $z \sim 2.3$ red-sequence color in Figure 6 by 0.16 mag (for a Calzetti et al. [2000] reddening law). The resulting evolution requires a later formation redshift, and this results in a slightly bluer color at low redshift. However, this effect is very small, and thus dust cannot be primarily responsible for the slow observed color evolution.

New starbursts in red-sequence galaxies (i.e., triggered by mergers) may reduce the color evolution. Birnboim et al. (2007) suggest that quenched galaxies may undergo a second starburst due to gas accretion. This starburst moves the galaxies back to the blue cloud. Once the star formation is quenched for the second time, the galaxy moves again to the red sequence. Compared to just passive evolution, the galaxy will be bluer due to the younger ages of the newly formed stars. In this context it is interesting to note that Labbé et al. (2007) find that episodic star-forming models provide the best explanation of the evolution of the blue sequence. Also, low-level residual star formation, or "frosting" of younger stars to an older "base" population, may depress the color evolution and could explain the apparently too-blue colors of the low-redshift red-sequence galaxies (see Trager et al. 2000). However, only $\sim$15% of the low-redshift field ellipticals show evidence for fairly recent star formation (e.g., Yi et al. 2005), and thus this effect cannot fully explain the slow color evolution.

An evolving IMF or metallicity may also alter the rest-frame $U - B$ evolution of the red sequence. For example, in case metallicity is lower for galaxies that form or quench at later times, $\Delta(U - B)$ will be slower. Furthermore, several authors have suggested that the IMF of massive elliptical galaxies may be top heavy or "bottom light" (see van Dokkum 2008 and references therein). Such IMFs lead to slower color evolution than Salpeter-like IMFs (Tinsley 1980), although the effect is relatively small (van Dokkum 2008). Finally, we note that the used stellar population models (Bruzual & Charlot 2003; Maraston 2005) might be incomplete, and the evolution in the models may be too strong.

6. SUMMARY

Our recent discovery of galaxies with quiescent stellar populations beyond $z = 2$ suggests that a red sequence is already in place at these redshifts. We examined this suggestion using our NIR spectroscopic survey of massive galaxies at $2 \lesssim z \lesssim 3$. The combination of spectroscopic redshifts and detailed continuum shapes as provided by the NIR spectra allows the first accurate rest-frame color and stellar mass determinations for a massive galaxy sample beyond $z = 2$.

The distribution of galaxies in the rest-frame $U - B$ color versus mass diagram demonstrates the existence of a red sequence at $z \sim 2.3$, with a significance of >3 σ. The red sequence hosts $\sim$60% of the stellar mass at the high-mass end ($>10^{11}$ $M_\odot$) at $z \sim 2.3$. We study the stellar populations of the red-sequence galaxies using emission-line diagnostics and stellar population modeling. The stellar continua, as provided by the NIR spectra, of nearly all red-sequence galaxies are best fit by specific SFRs of less than 0.05 Gyr^{-1}. Furthermore, in contrast to the blue galaxies, they have no detected rest-frame optical emission lines (e.g., Hα), or the line emission is dominated by AGN activity. Thus, both independent diagnostics imply that the red sequence is dominated by galaxies with quiescent stellar populations.

By combining rest-frame $U - B$ with $B - V$, we find that the $z \sim 2.3$ red-sequence galaxies are in a poststarburst phase, with typical ages of $\sim$0.5–1 Gyr. This finding is supported by the strong Balmer break in the stacked spectrum of all red-sequence galaxies. Overall, this implies that the red sequence is primarily driven by poststarburst galaxies at this epoch and probably has just started to build up at $z \sim 2.3$.

We study the rest-frame $U - B$ color evolution of massive galaxies by comparing our sample with spectroscopic galaxy samples at $z \sim 0.03$ and $\sim$0.73. Remarkably, rest-frame $U - B$ evolves slowly, by only $\sim$0.25 mag between $z \sim 2.3$ and the present. The fraction of massive galaxies ($>10^{11}$ $M_\odot$) on the red sequence increases by only $\sim$20% between $z \sim 2.3$ and $\sim$0.0. Similarly, the fraction of the total stellar mass of massive galaxies on the red sequence increases by only $\sim$15%. However, the number and mass density of the massive ($>10^{11}$ $M_\odot$) red-sequence galaxies grow by factors of $\sim$8 and $\sim$6, respectively, over the same redshift interval.

Overall, we show that the slow color evolution of the red sequence does not allow a straightforward explanation. Simple aging models predict a too-strong color evolution; consequently, the red-sequence galaxies are too red at $z \sim 0$. Also, such models cannot reproduce the strong density evolution of galaxies on the red sequence that we measure here. Presumably, the evolution is a combination of aging, galaxy transformations, and red mergers. Furthermore, frosting of young stars, recent starbursts, dust, and an evolving IMF may also play a minor role in the evolution of the red sequence, but this remains to be explored.

More accurate constraints on the color evolution require independent measurements of the metallicity, dust content, ages, current SFRs, and IMF of red-sequence galaxies over all epochs. As for the moment, the evolution of the number density and mass function provide the most powerful method to study the growth of the red sequence. The slope and spread (σ_{U-B}) can also be used to set further constraints on its buildup. However, due to the significant errors on the rest-frame colors and the small size of the $z \sim 2.3$ spectroscopic sample, we use neither in this work. We do note that none of the models discussed here violate the constraints imposed by the observed scatter.

Finally, we would like to note that our findings are supported by recent morphological studies. Using follow-up high-resolution NIC2 imaging on *HST* and adaptive optics imaging with NIRC2 on Keck, van Dokkum et al. (2008) find very compact sizes and extremely high inferred stellar mass densities for the red-sequence

galaxies in this paper (see also Trujillo et al. 2006, 2007; Toft et al. 2007; Zirm et al. 2007; Longhetti et al. 2007; Cimatti et al. 2008). This finding implies that these galaxies do not passively evolve into the red-sequence galaxies in the local universe. Thus, both the morphological and color evolution require active evolution to take place that transforms the $z \sim 2.3$ red-sequence galaxies to those at the current epoch.

We thank the members of the MUSYC collaboration for their contribution to this work. This research was supported by grants from the Netherlands Foundation for Research (NWO) and the Leids Kerkhoven-Bosscha Fonds. A. v. d. W. and G. D. I. acknowledge support from NASA grant NAG5-7697. Support from National Science Foundation CAREER grant AST 04-49678 is gratefully acknowledged.

REFERENCES

Adelman-McCarthy, J., et al. 2007, ApJS, 172, 634
Arnouts, S., et al. 2007, A&A, 476, 137
Bell, E. F., McIntosh, D. H., Katz, N., & Weinberg, M. D. 2003, ApJS, 149, 289
Bell, E. F., Phleps, S., Somerville, R. S., Wolf, C., Borch, A., & Meisenheimer, K. 2006, ApJ, 652, 270
Bell, E. F., et al. 2004, ApJ, 608, 752
Birnboim, Y., Dekel, A., & Neistein, E. 2007, MNRAS, 380, 339
Bower, R. G., Kodama, T., & Terlevich, A. 1998, MNRAS, 299, 1193
Bower, R. G., Lucey, J. R., & Ellis, R. S. 1992, MNRAS, 254, 601
Brammer, G., & van Dokkum, P. G. 2007, ApJ, 654, L107
Bruzual, G., & Charlot, S. 2003, MNRAS, 344, 1000
Bundy, K., Treu, T., & Ellis, R. S. 2007, ApJ, 665, L5
Calzetti, D., Armus, L., Bohlin, R. C., Kinney, A. L., Koornheef, J., & Storchi-Bergmann, T. 2000, ApJ, 533, 682
Cassata, P., et al. 2008, A&A, 483, L39
Chabrier, G. 2003, PASP, 115, 763
Cimatti, A., et al. 2008, A&A, 482, 21
Cirasuolo, M., et al. 2007, MNRAS, 380, 585
Conselice, C. J., et al. 2007, MNRAS, 381, 962
Drory, N., Salvato, M., Gabasch, A., Bender, R., Hopp, U., Feulner, G., & Pannella, M. 2005, ApJ, 619, L131
Elias, J. H., et al. 2006, Proc. SPIE, 6269, 139
Faber, S. M. 1973, ApJ, 179, 731
Faber, S. M., et al. 2007, ApJ, 665, 265
Fontana, A., et al. 2004, A&A, 424, 23
Förster Schreiber, N. M., et al. 2004, ApJ, 616, 40
Franx, M., & Illingworth, G. D. 1990, ApJ, 359, L41
Gawiser, E., et al. 2006, ApJS, 162, 1
Giavalisco, M., et al. 2004, ApJ, 600, L93
Kauffmann, G., et al. 2003, MNRAS, 341, 54
Kodama, T., & Arimoto, N. 1997, A&A, 320, 41
Kodama, T., Bower, R. G., & Bell, E. F. 1999, MNRAS, 306, 561
Kodama, T., et al. 2007, MNRAS, 377, 1717
Kriek, M., et al. 2006a, ApJ, 645, 44
———. 2006b, ApJ, 649, L71
———. 2007, ApJ, 669, 776
———. 2008, ApJ, 677, 219
Labbé, I., et al. 2005, ApJ, 624, L81
———. 2007, ApJ, 665, 944
Le Fèvre, O., et al. 2004, A&A, 428, 1043
Longhetti, M., et al. 2007, MNRAS, 374, 614
Maraston, C. 2005, MNRAS, 362, 799
Mignoli, M., et al. 2005, A&A, 437, 883
Papovich, C., et al. 2006, ApJ, 640, 92
Quadri, R., et al. 2007, AJ, 134, 1103
Reddy, N. A., et al. 2006a, ApJ, 644, 792
———. 2006b, ApJ, 653, 1004
Salpeter, E. E. 1955, ApJ, 121, 161
Schweizer, F., & Seitzer, P. 1992, AJ, 104, 1039
Shapley, A. E., Steidel, C. C., Erb, D. K., Reddy, N. A., Adelberger, K. L., Pettini, M., Barmby, P., & Huang, J. 2005, ApJ, 626, 698
Sirianni, M., et al. 2005, PASP, 117, 1049
Steidel, C. C., Giavalisco, M., Dickinson, M., & Adelberger, K. L. 1996a, AJ, 112, 352
Steidel, C. C., Giavalisco, M., Pettini, M., Dickinson, M., & Adelberger, K. L. 1996b, ApJ, 462, L17
Tinsley, B. M. 1980, Fundam. Cosm. Phys., 5, 287
Toft, S., et al. 2007, ApJ, 671, 285
Trager, S. C., Faber, S. M., Worthey, G., & González, J. J. 2000, AJ, 120, 165
Tran, K.-V. H., van Dokkum, P., Franx, M., Illingworth, G. D., Kelson, D. D., & Förster Schreiber, N. M. 2005, ApJ, 627, L25
Trujillo, I., Conselice, C. J., Bundy, K., Cooper, M. C., Eisenhardt, P., & Ellis, R. S. 2007, MNRAS, 382, 109
Trujillo, I., et al. 2006, ApJ, 650, 18
van der Wel, A., Franx, M., van Dokkum, P. G., Rix, H.-W., Illingworth, G. D., & Rosati, P. 2005, ApJ, 631, 145
van der Wel, A., et al. 2007, ApJ, 670, 206
van Dokkum, P. G. 2005, AJ, 130, 2647
———. 2008, ApJ, 674, 29
van Dokkum, P. G., & Franx, M. 2001, ApJ, 553, 90
van Dokkum, P. G., Franx, M., Kelson, D. D., Illingworth, G. D., Fisher, D., & Fabricant, D. 1998, ApJ, 500, 714
van Dokkum, P. G., et al. 2006, ApJ, 638, L59
———. 2008, ApJ, 677, L5
Vanzella, E., et al. 2006, A&A, 454, 423
Webb, T. M. A., et al. 2006, ApJ, 636, L17
White, M., et al. 2007, ApJ, 655, L69
Worthey, G. 1994, ApJS, 95, 107
Worthey, G., Faber, S. M., & Gonzalez, J. J. 1992, ApJ, 398, 69
Wuyts, S., et al. 2007, ApJ, 655, 51
———. 2008, ApJ, 682, 985
Yi, S. K., et al. 2005, ApJ, 619, L111
York, D. G., et al. 2000, AJ, 120, 1579
Zirm, A. W., et al. 2007, ApJ, 656, 66